Polymer Degradation and Stability 228 (2024) 110938

Contents lists available at ScienceDirect

Polymer Degradation and Stability

journal homepage: www.journals.elsevier.com/polymer-degradation-and-stability

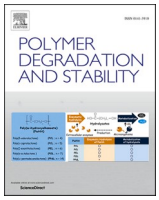

Polyamidoamine-based photostabilizers for cotton fabrics

Jenny Alongi , Sofia Treccani , Valeria Comite , Paola Fermo , Paolo Ferruti , Elisabetta Ranucci *

Dipartimento di Chimica, Università degli Studi di Milano, Via C. Golgi 19, 20133, Italy

A R T I C L E I N F O

Keywords:
Photoaging
Cellulose
Photostabilizers
Polyamidoamines

A B S T R A C T

Four water-soluble α-amino acid-derived polyamidoamines (PAAs) obtained by reacting N,N'-methylenebisacrylamide with glycine, leucine, arginine and glutamic acid were studied as photostabilizers of cotton. Untreated and PAA-treated cotton strips with 10 % PAA add-on underwent accelerated photoaging by UV irradiation in air at temperature from 25 to 50°C and 30 % relative humidity. Irradiation was applied in consecutive 4 h cycles, after each of which samples were analyzed by different techniques. After 30 h irradiation, the whiteness index and colorimetric parameters indicated significant yellowing of cotton, which became slightly more intense after 100 h irradiation. On irradiation, PAA-treated samples showed only slow decrease in whiteness and increase in yellowing. After 100 h, yellowing achieved significantly lower levels than in untreated cotton. In no case did the infrared spectroscopy and electron microscopy reveal detectable structural and morphological alterations, even after 100 h of UV exposure. Thermogravimetric analysis showed only little changes of thermograms following photoaging. X-ray diffraction analysis revealed slight deformation of the cellulose crystalline structure following both PAA treatment and UV irradiation. Finally, the PAA coatings were extracted from the cotton strips and analyzed by ^{1}H-NMR analysis. Only the glutamic acid-derived PAA showed detectable structural changes that did not involve the main chain. The FT-IR spectra and white indexes of the washed cotton strips did not differ from those of untreated cotton. Overall, it was proven that α-amino acid-derived PAAs protect cotton from photo-oxidation. Their performance was attributed to the radical scavenging ability of tert-amine groups present in their repeat units.

1. Introduction

One of the disadvantages of cellulosic materials, including cotton, linen and paper, is their tendency to undergo photoaging when exposed to air and light, particularly UV radiation [1]. This phenomenon causes discoloration, embrittlement and loss of aesthetic properties, and is significant in relation to the preservation of historical manuscripts and textiles, but also in materials science, due to the extensive use of cellulosic fibers in composite materials.

It is well known that the mechanism of the photoinduced decomposition of cellulose starts from the formation, under UV irradiation, of carbon-centered radicals, as demonstrated by electron spin resonance (ESR) tests. These form peroxyl radicals by reaction with oxygen, which can transform into hydroperoxides after hydrogen extraction [2]. These can in turn undergo homolytic decomposition to hydroxyl radical either under the effect of UV radiation in the spectral range below 360 nm [3,4], or due to the catalytic action of transition metal ions in the reduce form, such as for instance Fe^{2+} and Cu^{+} [4,5]. Due to their high reactivity, hydroxyl radicals react nonspecifically with carbohydrates and abstract hydrogen from C-H bonds [4]. UV exposure can introduce new functional groups, such as carbonyl and carboxyl groups, increasing the susceptibility of cellulose to degradation. Possible protection and mitigation strategies against photoaging of cellulose include addition of UV absorbers, reactive oxygen species (ROS) quenchers or antioxidants [6,7]. Additionally, since acidic conditions can exacerbate photoaging, deacidification treatments can help stabilize cellulose. Three main categories of photostabilizers based on UV absorbers can be identified, namely benzophenones [8], benzotriazoles [9] and triazines [10]. Benzophenones, such as for instance benzophenone-3 and benzophenone-4, absorb efficiently UV radiation in the 280-320 nm range. Benzotriazoles, including Tinuvin® P and Tinuvin® 327, protect against a broad range of UV wavelengths (280-400 nm). Examples of triazines used as UV absorbers include Cyasorb® UV-1164 and Cyasorb® UV-3638, known for their excellent photostability and efficiency. Hindered amine light stabilizers (HALS) do not absorb UV radiation but act as scavengers of free radicals formed during photooxidation, thus

* Corresponding author.
E-mail address: elisabetta.ranucci@unimi.it (E. Ranucci).

https://doi.org/10.1016/j.polymdegradstab.2024.110938
Received 9 July 2024; Received in revised form 26 July 2024; Accepted 1 August 2024
Available online 3 August 2024

Table 1
Experimental conditions adopted in the synthesis of PAAs.[a)]

PAA	α-amino acid	α-amino acid (g; mmol)	$LiOH{\cdot}H_2O$ (g; mmol)	Temperature (°C)	Time (days)
M-GLY	glycine	2.45; 32.32	1.38; 32.23	-	5
M-LEU	leucine	4.25; 32.07	1.37; 32.00	50	10
M-ARG	arginine	5.65; 32.11	-	50	9
M-GLU	glutamic acid	4.83; 32.17	2.70; 63.06	50	9

[a)] All preparations were performed using 5 g (32.11 mmol) N,N'-methylenebisacrylamide and 10 mL H_2O.

preventing degradation of cellulose [11]. Antioxidants such as phenolic and phosphite stabilizers are common additives used in conjunction with UV absorbers and HALS and provide a synergistic effect [12]. Phenolic stabilizers, such as butylated hydroxytoluene (BHT) are effective free radical scavengers. Phosphite stabilizers such as tris(nonylphenyl)phosphite (TNPP), decompose hydroperoxides formed during UV exposure. Although UV stabilizers are highly effective at protecting cellulose from UV radiation, they have some drawbacks and limitations that can affect their performance, environmental friendliness and costs. Particularly benzophenones and certain benzotriazoles, have been associated with potential health risks, including endocrine disruption and skin sensitization. Certain stabilizers can persist in the environment and accumulate in living organisms, raising concerns about long-term ecological effects. For example, some heterocyclic derivatives of benzotriazole represent an emerging threat, because they can be dangerous micropollutants, potentially mutagenic and carcinogenic [13].

Moreover, incorporating UV stabilizers into cellulosic materials can be challenging, particularly if they require specific processing conditions or are prone to leaching or migration. Thanks to their size, polymeric photostabilizers have lower volatility and extractability in solvents that induce environmental benefits, by reducing leaching and improving the safety profile of the final products [14]. They also improve workability and increase durability and thermal stability.

Polyamidoamines (PAAs) are synthetic polymers prepared by the aza-Michael polyaddition of prim- or sec- amines with bisacrylamides [15]. Most of the PAAs studied so far are water-soluble and the polymerization process preferably takes place at room temperature in water without added catalysts. Being a polyaddition reaction, the synthesis of PAAs does not involve the production of by-products. For all the above reasons, the synthetic process of PAAs can be considered green and easily scalable. PAAs are degradable in aqueous media [16], including physiological fluids, and are highly functional polymers that can be used for applications in different fields, for instance as substrates for tissue engineering [17], carriers for gene therapy [18], sorbents for water purification from heavy metal ions [19]. In addition, in the last decade, several bioinspired α-amino acid-derived PAAs have proved to be efficient flame retardants for cotton [20–23]. The same polymers did not exhibit significant phytotoxicity in seed germination tests [24,25] and aquatic toxicity in in vivo tests using zebrafish embryos (*Danio rerio*) as live animal models [26].

Since the thermo-oxidative decomposition of polymers proceeds through a radical mechanism, exactly as in photo-oxidative decomposition, it was hypothesized that PAAs could also play a role as photostabilizers. Therefore, in this study, a set of four PAAs obtained by the polyaddition of N,N'-methylenebisacrylamide with glycine (M-GLY), arginine (M-ARG), leucine (M-LEU) and glutamic acid (M-GLU) were studied for their ability to stabilize cotton from the action of UV radiation.

2. Experimental part

2.1. Materials

N,N'-methylenebisacrylamide (99 %), glycine (99 %), leucine (99 %), arginine (99 %), glutamic acid (98 %), lithium hydroxide monohydrate (98 %), and hydrochloric acid (HCl, 37 %) were supplied by Sigma-Aldrich (Milan, Italy) and used as received. Bleached cotton fabric (COT) with an area density of 220 g m^{-2} was purchased from Fratelli Ballesio S.r.l. (Turin, Italy).

2.2. Synthesis of polyamidoamines (PAAs)

Synthesis of M-LEU: N,N'-methylenebisacrylamide, leucine and lithium hydroxide monohydrate were dissolved in ultrapure water. The reaction mixture was heated to 50°C for 5 days in the dark under nitrogen. After this time, it was diluted to 25 mL with ultrapure water, the pH adjusted to 4.5 with 37 % HCl. The product was retrieved by freeze-drying the retained portion. All other PAAs were synthesized following the same procedure adopted for M-LEU, using the experimental conditions shown in Table 1.

2.3. Treatment of cotton fabrics with PAAs

Strips of cotton fabrics measuring 40 mm x 50 mm were dried at 100°C for 4 min and then weighed. Subsequently, the samples were impregnated with PAA aqueous solutions of 10 % concentration and dried at 100°C for 4 min. The total dry solid add-ons (*Add-on, wt.*- %) were determined weighing each sample before (W_i) and after (W_f) the impregnation step. The add-ons were calculated using Eq. (1):

$$Add-on = \frac{W_f - W_i}{W_i} \times 100 \quad (1)$$

For all PAAs, the final add-on was 10 %. PAA-treated cotton fabrics were coded as the following example: COT/M-GLY, which is the code for a cotton sample treated with 10 % add-on M-GLY.

2.4. Accelerated photoaging tests

The accelerated tests for investigating the photodegradation of samples were carried out inside a closed solar chamber, internally covered with aluminum foil. Samples of both untreated and PAA-treated samples (40 mm x 50 mm) were placed on a rotating stand and irradiated for a total of 100 h with a 250 W UV-A lamp (emission wavelength range: 315 - 400 nm) positioned 30 cm away from the sample holder. A 30 % relative humidity was obtained by placing a saturated $MgCl_2$ water solution in the chamber. Every 4 h, irradiation was interrupted for 1 h. During this time, samples were characterized by whiteness index measurements and colorimetric analyses. After each 4 h-irradiation cycle, the sample temperature varied from 25°C to 50°C, as measured using a Tilswall Digital thermometer (Germany) placed at a 15 cm distance from the fabric. At the end of the working day, samples were stored in the dark. All tests were performed in duplicate. At the end of the tests, PAA-treated cotton fabrics were extracted with water (50 mL) at room temperature for 30 min under stirring. The extracts were freeze-dried and the resultant white powders analyzed by ^{1}H-NMR in D_2O.

2.5. Characterization techniques

The chemical structure of M-GLY, M-LEU, M-ARG and M-GLU at 0 and 100 h of UV irradiation was assessed by ^{1}H-NMR, collecting

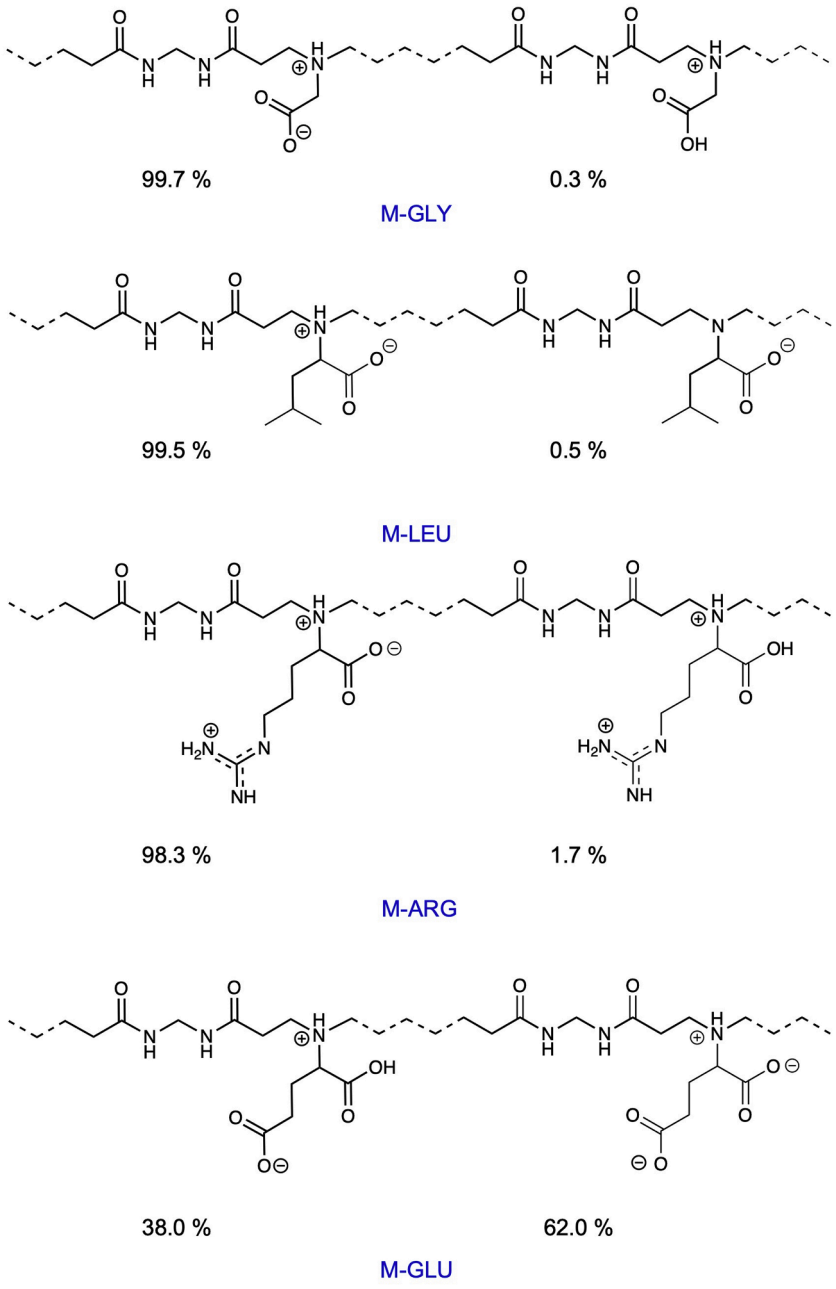

Fig. 1. Ionic species distribution of α-amino acid-derived PAAs at pH 4.5.

spectra in D_2O at pH 4.5 and at 25°C using a Bruker Advance DPX-400 NMR spectrometer (Milan, Italy) operating at 400.13 MHz. Parameters: scan number 32, relaxation delay, *d1*, 10.0 s, receiver gain automatically measured and set by the instrument.

Untreated cotton (COT) and PAA-treated cotton, namely COT/M-GLY, COT/M-LEU, COT/M-ARG and COT/M-GLU were analyzed at 0 and 100 h of UV irradiation by attenuated total reflectance (ATR) Fourier transform infrared spectroscopy (FT-IR). FT-IR/ATR spectra were recorded at room temperature, in the 4000 - 600 cm^{-1} wavenumber range, with 32 scans and 4 cm^{-1} resolution, using a Jasco FT-IR/FIR spectrophotometer (Milano, Italy), equipped with a ZnSe crystal characterized. After extraction from photoaged COT/M-GLU specimens, M-GLU was analyzed by using the same instrument.

The morphology of COT and COT/PAA samples at 0 h and 100 h of UV exposure were evaluated. The surface of untreated and PAA-treated fabrics (5 mm x 5 mm) was gold metallized and then analyzed with an EVO 15 scanning electron microscope (SEM) operating at 8.5 mm working distance and 5 kV beam voltage (Zeiss, Ramsey, NJ, USA). The X-ray diffraction (XRD) spectra of COT and COT/PAA samples were recorded using a Miniflex 600 diffractometer with Cu $K_{\alpha 1}$ radiation at 1.5405 Å, at 40 kV voltage and 15 mA current (Rigaku Europe SE, Germany). The thermal stability of COT and COT/PAA samples was assessed by thermogravimetric analysis (TGA) in nitrogen and air from 50 to 800°C range, at 10°C min^{-1} heating rate, with a 50 mL min^{-1} gas flow, using a TGA/DSC 2 Star System (Mettler-Toledo, Milan, Italy).

The effect of photodegradation of COT and COT/PAA samples following UV irradiation was evaluated by measuring their whiteness indexes and analyzing their color change by colorimetric analysis. The whiteness index (*WI*) was measured following the ISO 2469 standard [27], using a SA0835/OWM SAMA whiteness meter (SAMA Tools, Viareggio, Italy).

WI is determined based on the following Eq. (2) [28]:

Table 2
Average charge distribution on PAAs' repeat units.

PAA	pK_a values	IP	Net charge at pH 4.5 [a)]	Positive/Negative charge [a)]
M-GLY [22]	$pK_{a\text{-}COOH} = 1.9$ $pK_{a\text{-}\ NR3} = 7.7$	4.8	+0.003	1.003
M-LEU [31]	$pK_{a\text{-}COOH} = 2.11$ $pK_{a\text{-}NR3} = 7.37$	4.8	+0.005	1.005
M-ARG [22]	$pK_{a\text{-}COOH} = 2.2$ $pK_{a\text{-}\ NR3} = 6.4$ $pK_{a\text{-}guanidine} > 10$	9.7	+1.01	1.97
M-GLU [22]	$pK_{a\text{-}COOH,1} =$ 2.32 $pK_{a\text{-}COOH,2} =$ 4.28 $pK_{a\text{-}NR3} = 7.78$	3.3	-0.62	0.38

[a)] Data calculated from the charge distribution shown in Fig. 1.

$$WI = Y + 800\ \times (x_n - x) + 1700\ \times\ (y_n - y) \tag{2}$$

where Y is the Y-tristimulus value of the sample, x_n, y_n are the chromaticity coordinates of the perfect diffuser, and x, y the chromaticity coordinates of the sample, defined as Eq. (3):

$$x = \frac{X}{X+Y+Z};\quad x_n = \frac{X_n}{X_n+Y_n+Z_n} \tag{3}$$

$$y = \frac{Y}{X+Y+Z};\quad y_n = \frac{Y_n}{X_n+Y_n+Z_n} \tag{4}$$

And the parameters 800 and 1700 refer to the CIE standard illuminant D_{65}, a commonly used reference light source approximating average midday light in Western Europe, which is often taken as a standard for average daylight. Where X, Z and X_n, Z_n are the X and Z-tristimulus values of the sample and of the perfect diffuser, respectively. Results were reported as the average of three measurements.

Spectrophotometric measurements were performed following the ISO11664 standard [29], using a CM-2300d spectrophotometer (Konica Minolta, Guangzhou, China), the following parameters were obtained: color change (ΔE^*), chroma (C^*), hue (h^*) given by Eqs. (3)–(5):

$$\Delta E^* = \sqrt{(\Delta L^*)^2 + (\Delta a^*)^2 + (\Delta b^*)^2} \tag{5}$$

$$C^* = \sqrt{a^{*2} + b^{*2}} \tag{6}$$

$$h = arctg\frac{b^*}{a^*} \tag{7}$$

where L^* is the sample brightness, a^* and b^* are chromaticity coordinates, ΔL^*, Δa^*, and Δb^* are the differences of the brightness, a^* and b^* chromaticity coordinates of two samples. Both the chromaticity coordinates and the resulting ΔE^* do not have physical units, since they are abstract quantities that represent visual characteristics. ΔE^* is a measure on a perceptual scale that describes the difference in human color perception.

L^* ranges from 0 (black) to 100 (white) and indicates how light or dark the color is. C^* measures the vividness or intensity of color. Colors with low chroma values are less saturated and more neutral, while colors with great chroma values are saturated, appearing more intense. Hue indicates the direction of the color in the a^* - b^* plane and is expressed in degrees.

For each sample, measurements were performed in quintuplicate, and the resulting ΔE^* value was obtained as the average of five measurements. The higher the ΔE^*, the more the cotton has changed color during aging. Differences in color can be classified as: not present, if $\Delta E^* = 0$; not perceptible to the human eye, if $0 < \Delta E^* \leq 1$; perceptible through close observation, if $1 < \Delta E^* \leq 2$; immediately perceptible, if $2 < \Delta E^* \leq 10$; colors are more distinct, if $11 < \Delta E^* \leq 49$; colors are extremely different, if $\Delta E \geq 50$ [30].

3. Results and discussion

3.1. Water-soluble amphoteric polyamidoamines: synthesis and ionic species distribution

The objective of this study was to demonstrate the effectiveness of the α-amino acid derived PAAs coded M-GLY, M-LEU, M-ARG and M-GLU (Fig. 1 and Table 2) as photostabilizers of cotton. These PAAs contain in their repeat unit carboxyl groups besides tert-amine and amide groups. Therefore, they are amphoteric polyelectrolytes that present well-defined pH-dependent ionic species distributions. One of the research objectives was indeed to correlate the observed activity of PAAs to the average charge in the repeat units and the ratio between positive and negative charges. The PAAs of interest were synthesized according to a classical procedure by the aza-Michael polyaddition of N, N′-methylenebisacrylamide with the α-amino acids glycine, leucine, arginine and glutamic acid (Scheme 1), in a 1:1 mole ratio. The synthetic process was carried out in a pH 11 water solution, at a 50 wt. % solid concentration and different reaction times, due to the different reactivities of α-amino acids caused by the different steric hindrance of the side substituents [15]. The raw products were retrieved by freeze-drying with no further purification. The chemical structures of the final products were confirmed by ^{1}H-NMR spectroscopy (Figs. S1–S4, respectively,

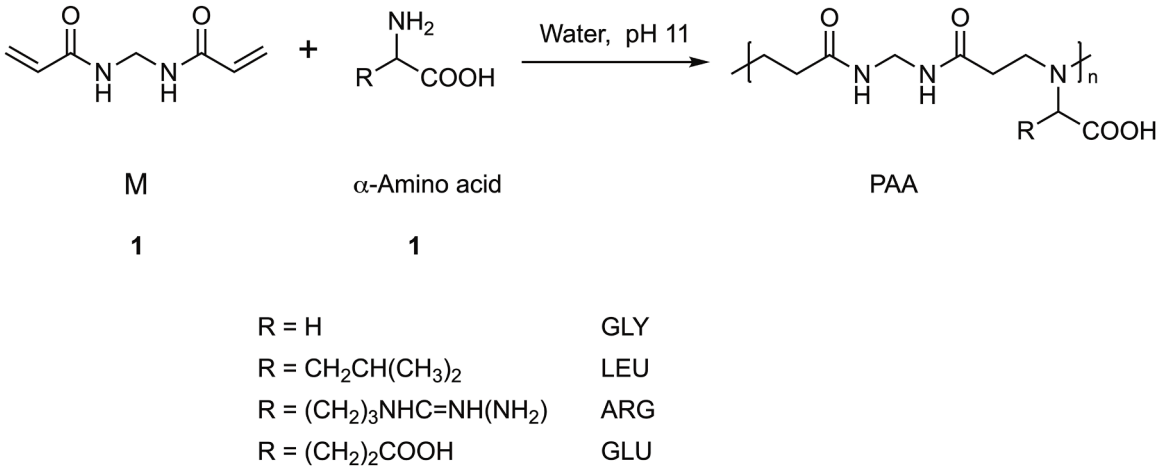

Scheme 1. Synthesis of M-GLY, M-LEU, M-ARG and M-GLU.
For the sake of simplicity, charges have been omitted.

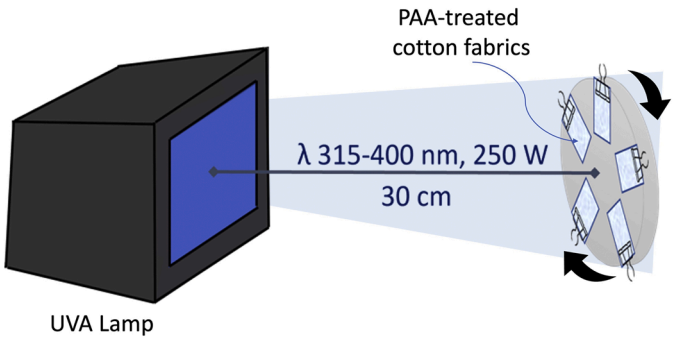

Fig. 2. Sketch of the interior of the closed chamber used in accelerated photoaging tests.

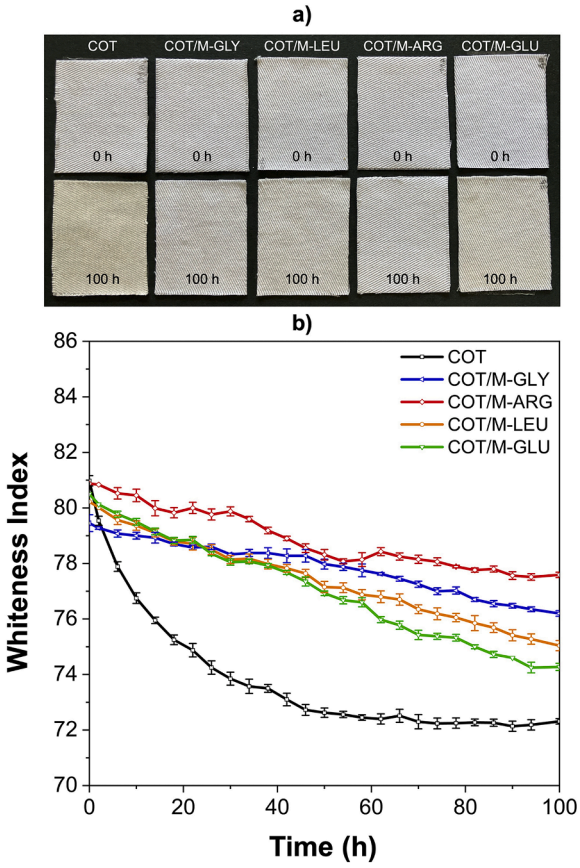

Fig. 3. Appearance (a) and whiteness index (b) of untreated and PAA-treated cotton fabrics subjected to accelerated photoaging. All measurements were carried out orientating the whiteness index meter along the same direction.

in Supplementary Materials). The number average molecular weights, calculated from the ^{1}H-NMR spectra from the ratio between the integrals of the resonance peaks relative to the internal units and the integrals of the resonance peaks relative to the terminal repeat units, were 10000, 2500, 4000 and 3200 for M-GLY, M-LEU, M-ARG and M-GLU, respectively.

The pK_a values of the ionizable functions present in PAAs and their isoelectric points, *IP*, (Table 2) are consistent with the presence in their repeat units at pH 4.5, at which their water solutions are used to impregnated cotton, of a slight excess positive charge in M-GLY and M-LEU, an overall negative charge in M-GLU, and an overall positive charge in M-ARG. The speciation curves obtained from the pK_a values of PAAs (Figs. S5–S8) allowed obtaining the distribution of the ionic species shown in Fig. 1. As stated above, M-GLY and M-LEU feature an almost perfect balance of ionic species with opposite charge, whereas M-GLU is highly anionic and features 62 % repeat units with two negative charges and one positive charge, the remaining being zwitterionic (net average charge per repeat unit -0.62; positive/negative charge ratio 0.38). M-ARG features 98.3 % repeat units with two positive charges and one negative and only 1.7 % repeat units with two positive charges (net average charge per repeat unit +1.01, positive/negative charge ratio 1.97).

Accelerated UV-aging tests

Photoaging tests were carried out on cotton fabrics impregnated with PAA aqueous solutions at pH 4.5, which represents the condition of maximum stability of PAAs [16], and then dried. Experiments with a 10 % add-on were conducted with all PAAs. As described in Section 2.4, accelerated tests were carried out by exposing PAA-treated cotton specimens to extensive UV-A irradiation in air within a closed chamber whose internal surfaces were coated with a reflecting surface at 30 % relative humidity (Fig. 2). The irradiation proceeded through consecutive 4 h-cycles, and were followed by a 1 h-rest, during which time the FT-IR spectra, the whiteness indexes and the reflectance spectra of the samples were recorded to monitor any structural and color changes in the samples. At the end of the working day, samples were stored in the dark. All samples were subjected to a total of 100 h irradiation. At the end of the each 4 h-irradiation cycle, the sample temperature raised up to 50°C. Pictures of untreated and PAA-treated cotton samples before and after aging are shown in Fig. 3a.

No changes in the FT-IR spectra of the PAA-treated cotton were observed even after 100 h irradiation (Fig. S9), revealing that no profound structural change was induced by photoaging under the selected conditions.

3.2. Whiteness measurements

Whiteness is defined as the measure of how closely the optical properties of a surface approximate the properties of a perfectly reflective surface, which neither absorbs nor transmits light but reflects it with equal intensity in all directions [32]. The whiteness index of a fabric quantifies the amount of light it reflects in the visible light spectrum and is related to how white it appears to the human eye. Therefore, it is an important parameter to assess the quality of white fabrics in textile industry, because the white color is associated to neatness. The whiteness index can be defined based on the International Commission for Illumination (CIE), as shown in Eq. (2) (Section 2.5). Whiteness measurement is expressed on a scale of 1-100, with 100 being the value that corresponds to a perfect white. Aging of an integer, bleached cotton textile induces formation of UV-absorbing chemical functions on fiber surfaces and causes yellowing. Therefore, in this study, the effect of the PAA coating on cotton aging was first monitored by measuring the dependence of the whiteness index of the PAA-treated cotton specimens on the UV exposure time, taking as a reference the change in the whiteness index of untreated cotton specimens subjected to the same irradiation in the same conditions. Photoaging of cotton samples was monitored by measuring the decrease of the whiteness index after each 4 h-cycle of irradiation. All measurements were carried out orientating the whiteness index meter along the same direction. It is indeed well-known that the optical properties of fabrics, particularly cotton, are different along these two directions due to a combination of fiber and yarn characteristics, including different density and porosity, different texture, as well as different optical properties, for instance due to the angle of light incidence. The UV irradiation time dependence of the *WI* for untreated and PAA-treated cotton samples with 10 % PAA add-on is shown in Fig. 3b. It can be observed that untreated cotton samples showed a substantial *WI* reduction until 30 h irradiation from 81.0 to 73.9, undergoing only slight changes for the remaining part of the

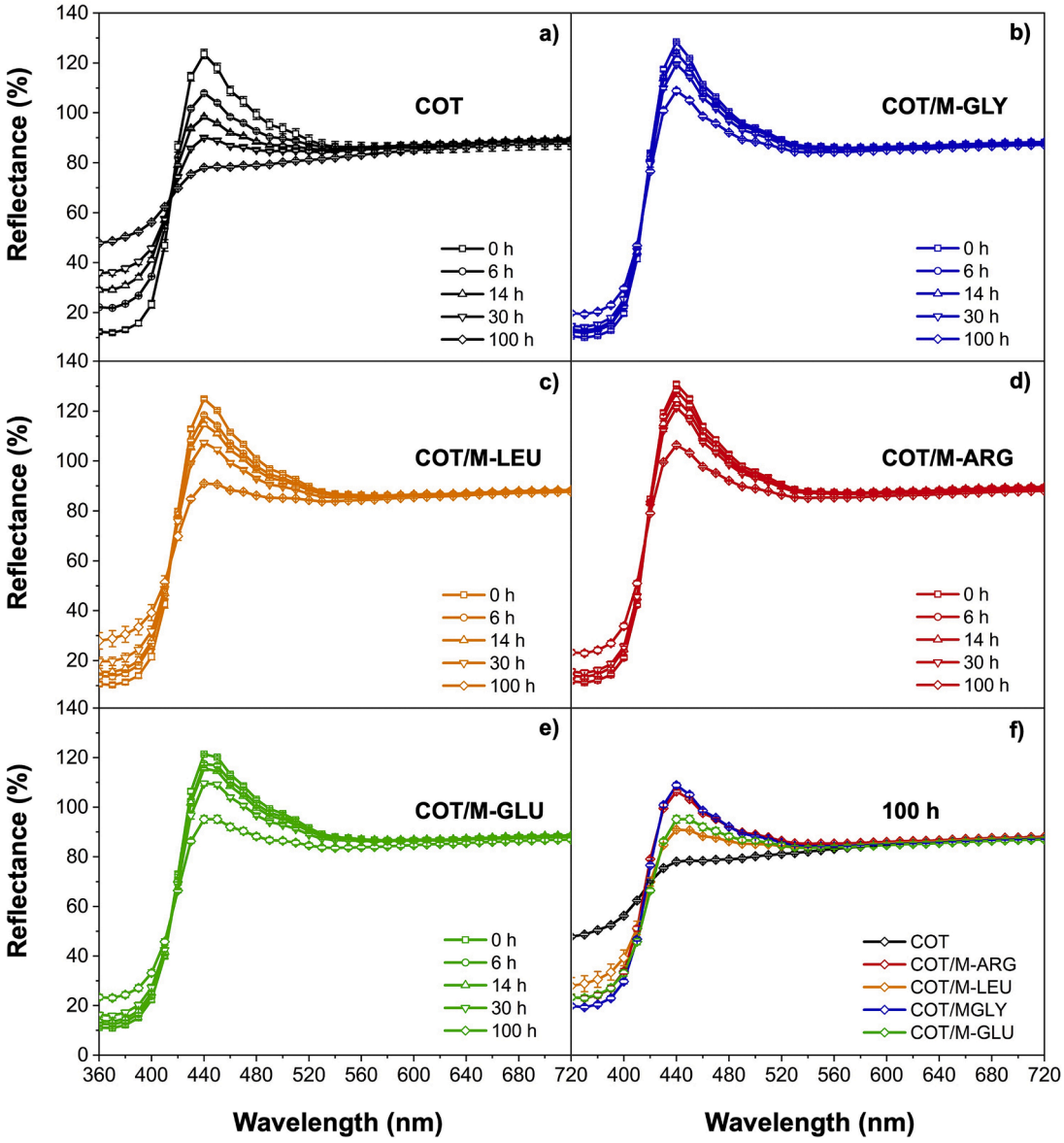

Fig. 4. Reflectance spectra of untreated and PAA-treated cotton fabrics at different photoaging stages.

experiment. Conversely, the *WI* of the PAA-treated samples decreased almost linearly with the irradiation time, until reaching final values at 100 h irradiation from 74.3 to 77.6, that is, significantly higher than that of untreated cotton (*WI* = 72.3). The PAA performance wase ranked in the order: M-ARG > M-GLY > M-GLU > M-LEU.

3.3. Colorimetric analysis

The photoaging of untreated and PAA-treated cotton was further studied by analyzing the color change of the samples following UV irradiation using a reflectance spectrophotometer. Reflectance spectra in the 350-725 nm range were recorded after each 4 h-cycle of irradiation, in parallel to whiteness index measurements and FT-IR analyses. Reflectance spectra were recorded on samples always oriented along the same axis. Representative results obtained for both untreated and PAA-treated cotton after different irradiation times are shown in Fig. 4. It can be observed that the maximum reflectance value of cotton, placed at 440 nm, dropped fast already after the first irradiation cycles, reducing reflectance from 124 to 90 % after 30 h irradiation, and finally reaching approximately 78 % after 100 h irradiation (27 and 37 % reduction, respectively). The maximum reflectance values of the PAA-treated samples at 440 nm decreased much more slowly, from 128 to 120 % for M-GLY, from 125 to 107 % for M-LEU, from 130 to 125 for M-ARG, and from 121 to 110 % for M-GLU after 30 h irradiation, and to 109, 91, 106, and 95 %, respectively, after 100 h irradiation. The PAA performance was ranked in the order: M-GLY (-15 % reflectance) > M-ARG (-18 %) > M-GLU (-22 %) > M-LEU (-27 %).

To better analyze the color changes of photoaged cotton samples, the irradiation time dependance of the CIELAB chromatic parameters, namely color change, ΔE^*, chroma, C^*, lightness, L^*, chromaticity coordinates a^*, b^*, and hue, h^*, as defined in Eqs. (5)–(7) (Section 2.5) was studied. The CIE L^*, a^*, b^* color space, also called CIELAB, encompasses the range of human color perception and distinguishes color differences using three color values. L^* value varies from 0 (black) to 100 (white), whereas a^* and b^* values have positive or negative values to indicate a chromatic color. In fact, positive a^*, negative a^*, positive b^*, and negative b^* indicate redness, greenness, yellowness and blueness respectively. If $a^* = b^* = 0$, the color is an achromatic color. Accordingly, the perfect colorless white has the values L^* =100, $a^* = 0$, $b^* = 0$, and $C^* = 0$. The results collected for both untreated and PAA-treated

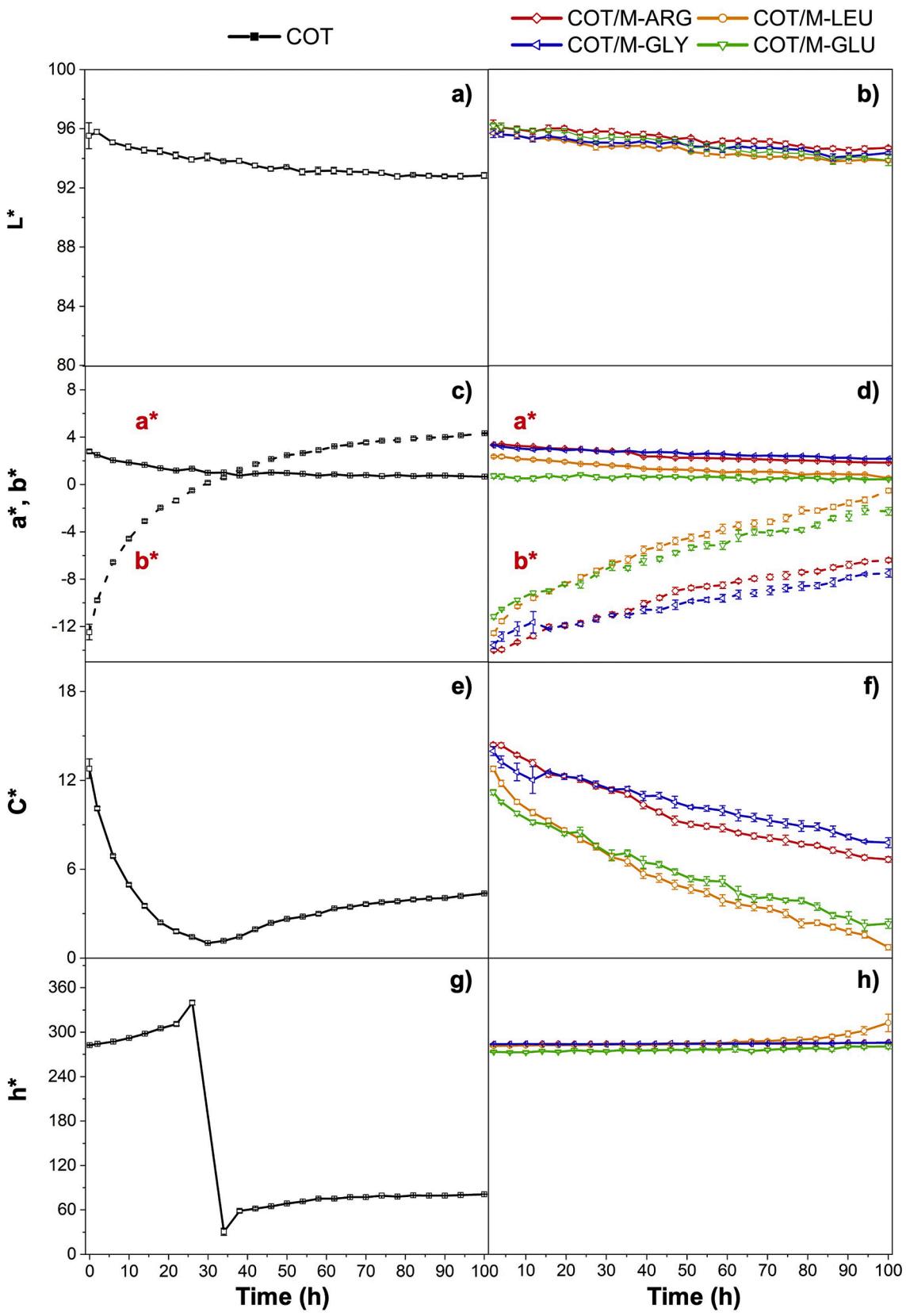

Fig. 5. Change of the color parameters of untreated and PAA-treated cotton during accelerated photoaging. L^* = lightness; a^*, b^* = chromaticity coordinates; C^* = chroma; h^* = hue. The definition of these parameters is given in Section 2.5.

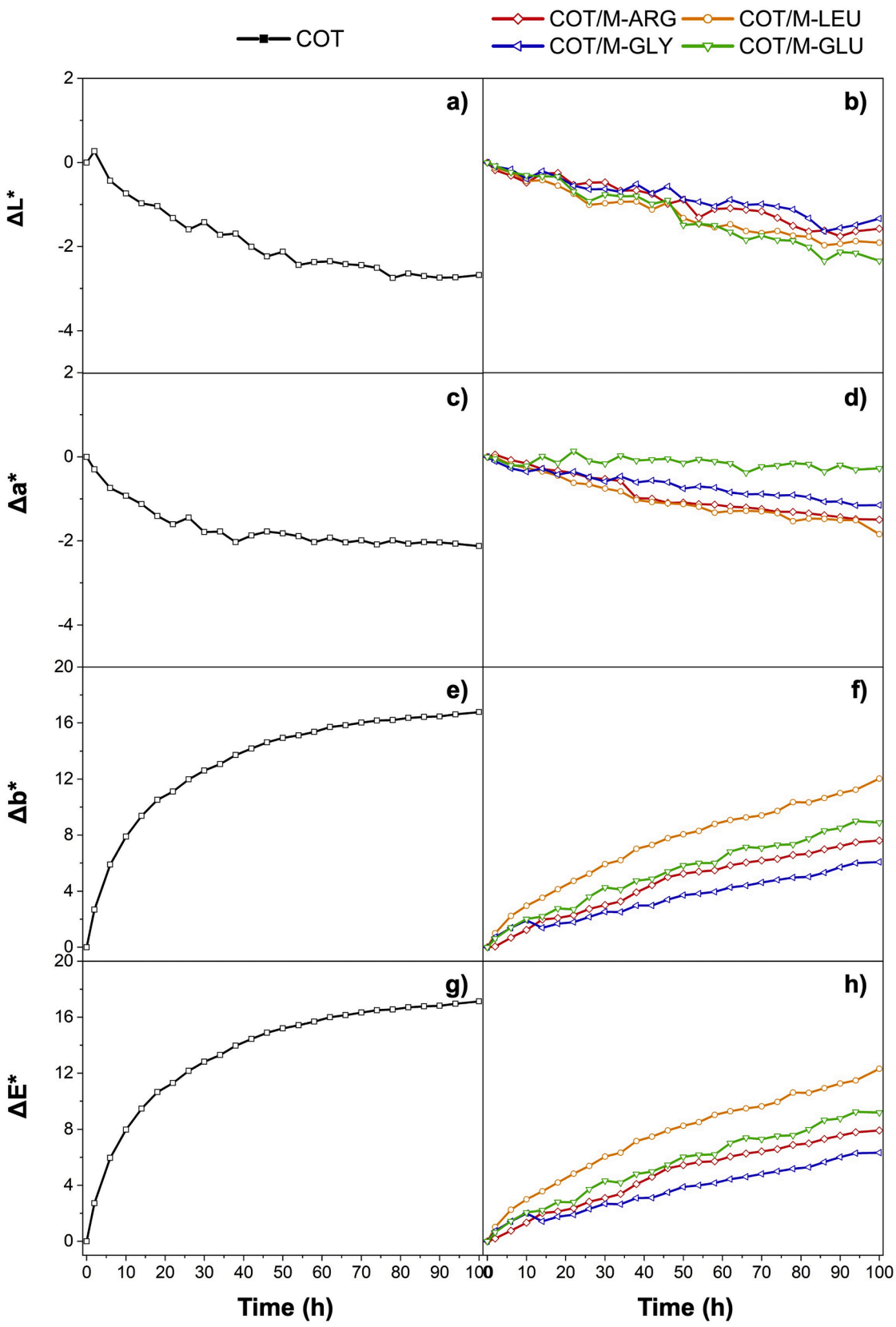

Fig. 6. Change of the color parameters of untreated and PAA-treated cotton during accelerated photoaging. ΔE^* = color change; ΔL^*, Δa^* and Δb^* = difference between the brightness and chromatic coordinate values, respectively, measured after each irradiation time and the values of the same parameters measured before the start of irradiation. The definition of these parameters is given in Section 2.5.

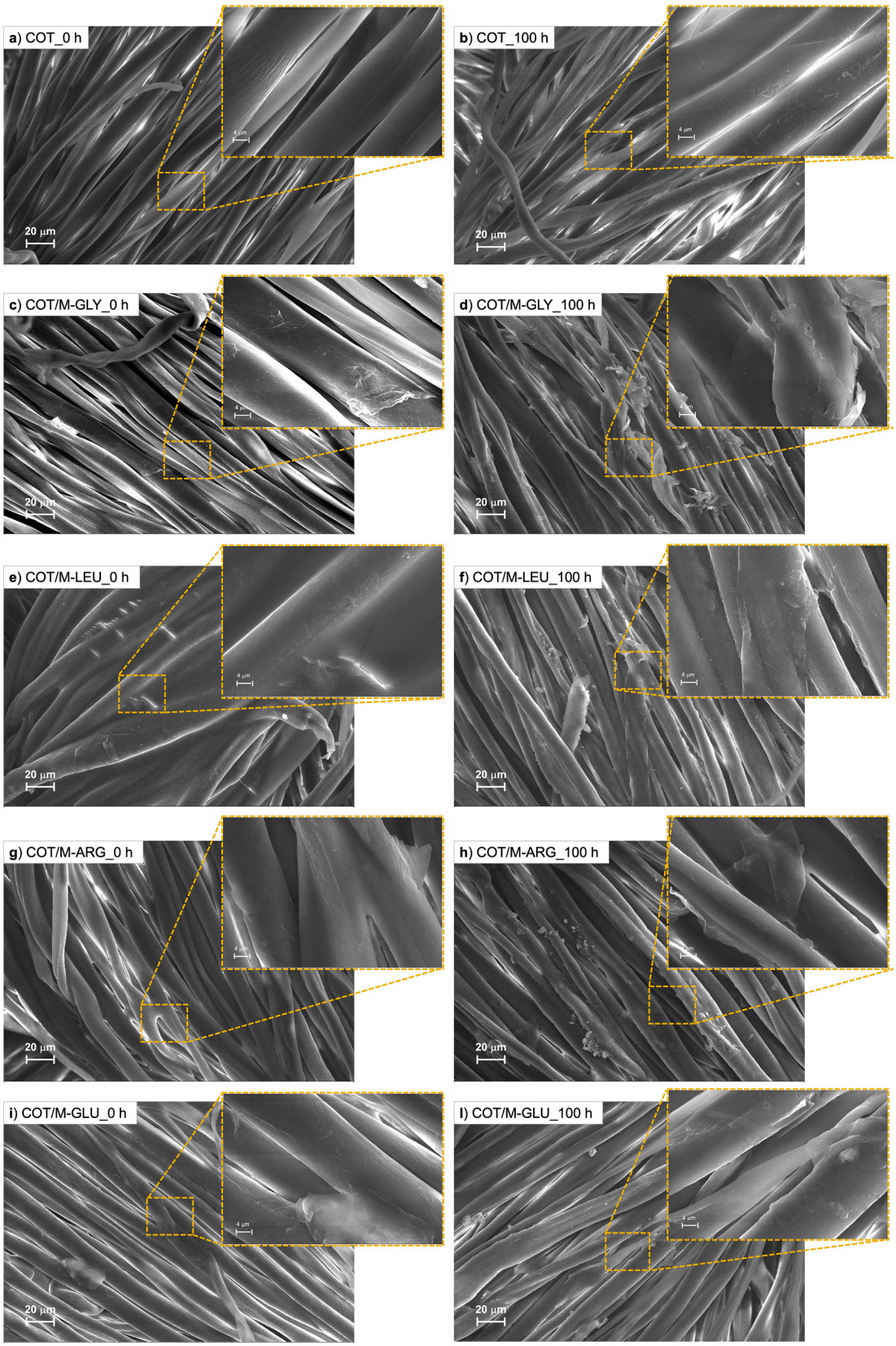

Fig. 7. SEM micrographs in secondary electron mode (1000X) of untreated cotton (COT) and cotton fabrics treated with 10 % add-on M-GLY, M-LEU, M-ARG, and M-GLU after 0 h (**a, c, e, i**) and 100 h UV irradiation (**b, d, f, l**). Insert magnification: 5000X.

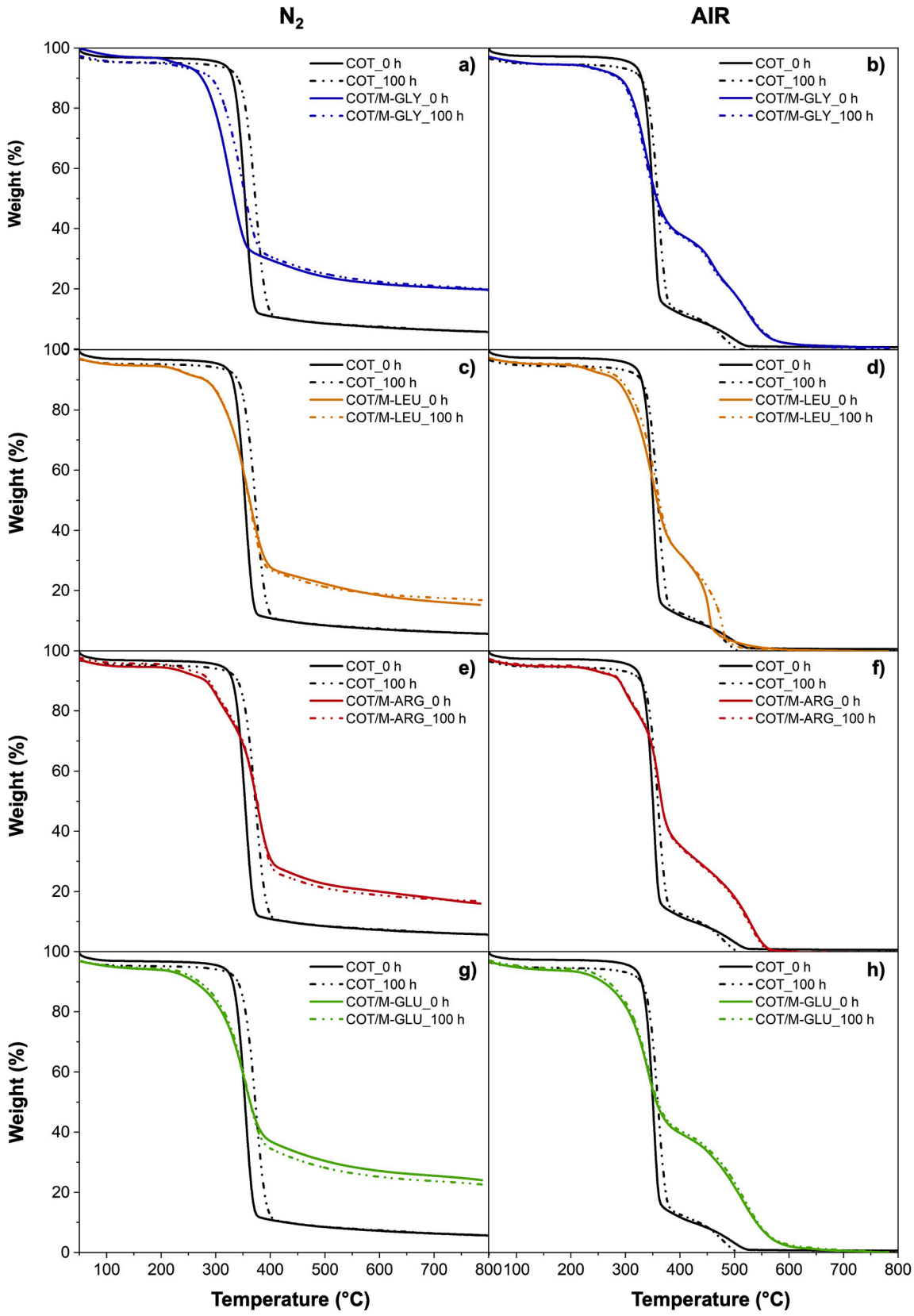

Fig. 8. TG thermograms of untreated and PAA-treated cotton fabrics in nitrogen (**a, c, e** e **g**) and in air (**b, d, f e h**) at 0 and 100 h UV irradiation. PAA add-on = 10 %.

cotton samples are shown in Fig. 5. The trends of ΔL^*, Δa^* and Δb^*, calculated as the difference between the values of the parameters measured after different irradiation times and those of the same samples before they were subjected to irradiation, as well as ΔE^*, calculated from Eq. (5), are shown in Fig. 6. It can be observed that in all cases studied the brightness value, L^*, decreases linearly and slowly with the irradiation time (Fig. 5a and b), a little faster in the case of untreated cotton, reaching a ΔL^* value of approximately -3 for untreated cotton and approximately -1.8, on average, for PAA-treated cotton samples after 100 h of irradiation (Fig. 6a). The a^* chromaticity coordinate also varied linearly and with an even slower rate than L^* both for untreated and PAA-treated cotton, with a slightly higher rate for the untreated sample (Fig. 5c and d). The trend of the b^* chromaticity coordinate was significantly different. In untreated cotton, b^* increased significantly within the first 30 h irradiation, passing from -12.5 to +0.1, the latter value indicative of a significant yellowing, and the, reaching +4.3 after 100 h irradiation (Fig. 5c and d). Conversely, in PAA-treated cotton samples, the b^* coordinate increased linearly and slowly with the irradiation time, passing from minimum values of -13.6, -12.6, -14.0, and -11.2 for M-GLY, M-LEU, M-ARG, M-GLU, respectively, to maximum values of -7.5, -0.6, -6.4, and -2.3 at 100 h, respectively, not reaching positive values and remaining much lower than the values achieved by cotton. Interestingly, being the irradiation time the same, both untreated cotton and PAA-treated cotton showed almost the same values of ΔE^* and Δb^* (Fig. 6e–h). Again, the PAA efficacy could be ranked as: M-GLY≈ M-ARG >> M-GLU > M-LEU, as revealed by the progressive increase of the slope of the ΔE^* and Δb^* curves with the irradiation time (Fig. 6e–h).

Interesting deductions could be drawn from the analysis of the dependence of the color intensity, C^*, on the irradiation time (Fig. 5e and f). The a^* and b^* curves of untreated cotton feature a cross-over point at 34 h irradiation, corresponding to a change in the relative contribution of the chromaticity coordinates, above which $b^*/a^* > 1$ and the yellow component of the color becomes relevant. At the cross-over point, the C^* value reaches a minimum value since $b^*/a^* = 1$. This corresponds to a discontinuity and a sudden decrease of the hue, h^*, expressed as the arctangent b^*/a^*, to 45° (Fig. 5g and h). In the case of PAA-treated cotton samples, no cross-over points were observed within the duration of the experiment and the C^* values increased linearly and slowly with the irradiation time. For this reason, the h^* values remain almost constant for the entire experiment duration. By extrapolation of the a^* and b^* curves, cross-over values of approximately 115 for M-LEU-, 134 for M-GLU-, and 240 h for M-ARG- and M-GLY-treated cotton samples, respectively, were estimated.

3.4. Efficacy of PAAs as photostabilizers for cotton

The efficacy as anti-photoaging coatings of cotton of the PAAs presented in this study can be ascribed to their action as antioxidants and radical scavengers. The role of radical scavengers is indeed to react with the reactive oxygen species (ROS) formed during the photooxidation of cellulose blocking them and preventing their further oxidation with cellulose [33]. PAAs do not normally absorb UV-A rays, unless specific chromophores are introduced in their repeat units, and are generally thermally stable and resistant to oxidation. In fact, amide bonds present in their main chain are particularly stable to radical reactions and oxidation. It is reasonable to assume that the activity of PAAs as radical scavengers is due to the ability of the tert-amine groups present in their main chain to react with radicals by donating their lonely electron pairs, and form less reactive species [34]. The fact that at the working pH, i.e. pH 4.5, all tert-amines are protonated does not inhibit their activity, due to dynamic deprotonation/protonation equilibrium involving these groups. In addition, all PAAs considered in this work bear, besides amide groups, other electron-withdrawing functions, namely carboxyl groups. Therefore, in case radicals are formed by abstraction of α hydrogens, they are stabilized by resonance delocalization.

Table 3
Thermal data of COT/PAA samples in nitrogen and air by thermogravimetric analysis.

Sample	Exposure time (h)	$T_{onset10\%}$ [b] (°C)	T_{max1} [c] (°C)	T_{max2}, T_{max3} [d] (°C)	RMF_{800} [e] (%)
Nitrogen					
COT	0	331	357	-	6
	100	340	371	-	6
COT/M-GLY [a]	0	274	326	-	20
	100	291	347	-	20
COT/M-LEU [a]	0	280	357	-	15
	100	281	361	-	17
COT/M-ARG [a]	0	282	375	-	16
	100	288	378	-	17
COT/M-GLU [a]	0	260	353	-	24
	100	269	357	-	23
Air					
COT	0	329	350	492	0
	100	328	359	481	0
COT/M-GLY [a]	0	289	336	460, 523	0
	100	286	337	469,529	0
COT/M-LEU [a]	0	282	347	456	0
	100	291	358	479	0
COT/M-ARG [a]	0	289	361	529	0
	100	290	360	528	0
COT/M-GLU [a]	0	258	342	515	0
	100	268	343	522	0

[a] Add-on ± 0.5 %. [b] Onset decomposition temperature at 10% weight loss. [c] First temperature at maximum weight loss rate in the 300 - 400°C range (step 1). [d] Second and third temperature at maximum weight loss rate in the 350 - 500°C (step 2) and 500 - 600°C (step 3) range, respectively. [e] Residual mass fraction at 800°C.

As regards relative efficacy, the analysis of the color coordinates of untreated and PAA-treated cotton samples following UV irradiation point to the same conclusion: M-GLY ≈ M-ARG >> M-GLU > M-LEU, with a clear gap in the efficacy of the first and the second couple of polymers. This behavior can be related to the different susceptibility of PAAs to radical reactions. Higher reactivity can indeed destabilize PAA structure and generate radicals that can trigger cotton decomposition. M-GLY is the most stable PAA in radical reactions, since it has the lowest content of hydrocarbon moieties and does not contain tertiary hydrogens, but only methylene groups, which are poorly reactive in radical reactions. M-ARG has only one mobile tertiary hydrogen α to the carboxyl group and, additionally, the guanidine residue can efficiently stabilize radicals by resonance. The lower efficacy of M-GLU can be explained considering that it contains two carboxyl groups and, therefore, is more susceptible to participating in radically induced decarboxylation reactions. Finally, the lower efficacy of M-LEU can be ascribed to the presence, in the repeat units, of a radical-sensitive isopropyl side substituent, due to presence of a tertiary hydrogen α to two alkyl groups that stabilize radicals thanks to their positive inductive effect.

3.5. Morphological analysis

The effect of the exposure to UV irradiation on the surface morphology of the PAA-treated cotton specimens was studied by scanning electron microscopy (SEM). Fig. 7 shows the morphologies of untreated and PAA-treated cotton fabrics at 1000X and 5000X magnification at 0 h and after 100 h of UV irradiation. Fibers of both

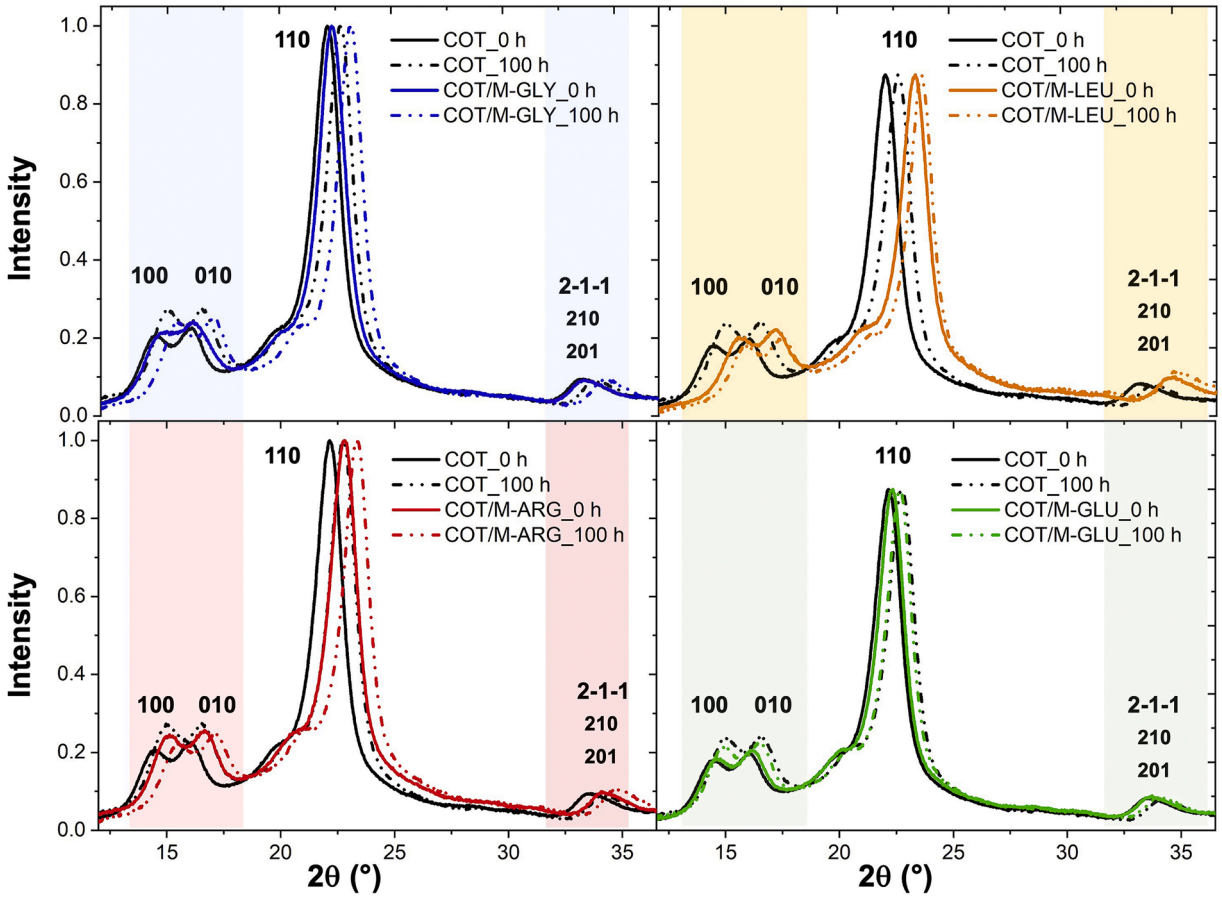

Fig. 9. XRD spectra of untreated cotton (COT) and cotton fabrics treated with 10% add-on M-GLY (**a**), M-LEU (**b**), M-ARG (**c**), and M-GLU (**d**) after 0 and 100 h UV irradiation.
The 1_t - 4_t peaks are ascribed to the glycine-based terminals. The green asterisks indicate traces of the vinyl-based terminals. Small changes in the positions of the 1-4 resonance peaks are due to the pH-dependence of the PAA proton magnetization.

untreated and PAA-treated cotton maintained the original spiralization of cellulose fibrils, a generally flat and smooth surface, but with a significant level of inhomogeneities related to its natural origin. SEM did not reveal detectable structural changes, even after 100 h of UV exposure

3.6. Effect of photoaging on the thermal stability of cotton and PAA-treated cotton fabrics

The effect of accelerated photoaging on the thermal and thermo-oxidative stability of cotton and PAA-treated cotton samples was investigated by thermogravimetric analysis (TGA) in nitrogen and air (Fig. 8) in the range 50-800°C. Relevant thermal data, including onset

Table 4
Position of XRD signals and crystallographic parameters of photoaged PAA-treated cotton samples.

Sample	2θ (°) [a] *(shift with respect to cotton)* [b]			d (nm) [c] *(change with respect to cotton)*			X_{cr} (%) [d]
Assignment	100	010	110	100	010	110	
After 0 h UV irradiation							
Cotton	14.64	15.94	22.14	0.305	0.280	0.204	57
COT/M-GLY	15.04 *(+0.40)*	16.12 *(+0.18)*	22.36 *(+0.22)*	0.297 *(-0.008)*	0.277 *(-0.003)*	0.202 *(-0.002)*	59
COT/M-LEU	15.60 *(+0.96)*	17.30 *(+1.36)*	23.48 *(+1.34)*	0.286 *(-0.018)*	0.259 *(-0.021)*	0.193 *(-0.011)*	54
COT/M-ARG	15.26 *(+0.62)*	16.70 *(+0.76)*	22.78 *(+0.64)*	0.293 *(-0.012)*	0.268 *(-0.012)*	0.199 *(-0.005)*	55
COT/M-GLU	14.64 *(0.00)*	16.08 *(+0.14)*	22.34 *(+0.22)*	0.305 *(0.00)*	0.278 *(-0.002)*	0.203 *(-0.001)*	56
After 100 h UV irradiation							
Cotton	14.96	16.56	22.74	0.298	0.270	0.199	58
COT/M-GLY	15.42 *(+0.46)*	17.0 0 *(+0.04)*	23.22 *(+0.48)*	0.290 *(-0.009)*	0.263 *(-0.007)*	0.195 *(-0.004)*	58
COT/M-LEU	15.82 *(+0.86)*	17.48 *(+0.92)*	23.78 *(+1.04)*	0.283 *(-0.016)*	0.256 *(-0.014)*	0.191 *(-0.008)*	54
COT/M-ARG	15.56 *(+0.60)*	17.10*(+0.54)*	23.34 *(+0.60)*	0.287 *(-0.011)*	0.262 *(-0.008)*	0.194 *(-0.005)*	53
COT/M-GLU	14.94 *(-0.02)*	16.56 *(0.00)*	22.68 *(-0.06)*	0.299 *-0.001)*	0.270 *(0.00)*	0.200 *(+0.00)*	57

[a] Diffraction angle. [b] The difference in value in relation to cotton is given in brackets. [c] Interplanar distance, calculated from 2θ values using the Bragg law equation $d = sin\theta/n\lambda$, where n (diffraction order) $=1$, $\lambda =$ radiation wavelength. [d] Degree of crystallinity, calculated from the ratio of the overall crystallinity peak area to the sum of the crystallinity peak areas plus amorphous aloe [37].

Table 5
Whiteness index (WI) values of PAA-treated cotton samples before and after PAA extraction.

Sample	*WI* after 0 h UV irradiation	*WI* after 100 h UV irradiation	*WI* after PAA extraction
COT	81.0 ± 0.2	72.3 ± 0.2	-
COT/M-GLY	79.5 ± 0.3	76.2 ± 0.2	78.6 ± 0.7
COT/M-LEU	80.2 ± 0.2	75.0 ± 0.2	79.9 ± 0.4
COT/M-ARG	80.9 ± 0.2	77.6 ± 0.2	78.5 ± 0.7
COT/M-GLU	80.5 ± 0.2	74.3 ± 0.2	79.1 ± 0.7

decomposition temperature (temperature at 10 % dry weight loss, $T_{onset10}$ %), temperature at maximum weight loss rate, T_{max}, and residual mass fraction, RMF_{800}, measured at 800°C and expressed as a percentage of the original weight, are shown in Table 3. The effect of PAAs on the thermal and thermo-oxidative stability of cotton was previously described for all the investigated PAAs [20,21]. In nitrogen (Fig. 8a), the trend of the weight loss curve of all PAA-treated cotton samples with 10 % PAA add-on was qualitatively like that of untreated cotton that showed one single major weight loss. However, the $T_{onset10\%}$ and T_{max1} values shifted to lower temperatures, and the residual mass fractions detected above 350°C significantly increased in all the PAA-treated sample (Table 3). In air (Fig. 8b), the TG curve of untreated cotton showed two inflections, placed at 342 and 472°C, and the residual mass fraction dropped rapidly to 0 % from 350 to 500°C. The PAA coating induced a shift of the $T_{onset10}$ % and T_{max1} values to lower temperatures, as well as an increase of the residual mass fraction above 350°C. Meanwhile, the T_{max2} value remained almost unchanged. Interestingly, the addition of 10 % PAAs did not induced significant changes of the TG patterns of the photoaged cotton samples both in nitrogen and in air. Except for M-GLY-coated cotton, which exhibited a moderate shift upward of both $T_{onset10}$ % and T_{max1} in nitrogen, all other curves were superimposable to those obtained before the start of photoaging. The TG curve of untreated cotton exhibited an upward shift of T_{max1} in nitrogen.

3.7. Effect of photoaging on the crystallinity of cotton and PAA-treated cotton fabrics

The effect of accelerated photoaging on the crystalline structure of cellulose in untreated and PAA-treated cotton samples was investigated by X-ray diffraction (XRD) analysis. The XRD patterns of untreated and PAA-treated cotton samples after 0 and 100 h UV irradiation and the relevant parameters of cellulose crystallinity are shown in Fig. 9 and Table 4, respectively.

The diffraction spectrum of cellulose in untreated cotton before irradiation shows the typical strong and broad diffraction peaks at 14.96°, 15.94° and 22.14° attributed to the (100), (010), (110) and (2-1-1)/(210)/(201) crystal facets of cellulose, as well as a shoulder around 20° attributed to the (012)/(102) facets and a the less intense broad peak centered at 33.68° attributed to the (2-1-1)/(210)/(201) crystal facets [35,36]. Under the effect of photoaging, the spectra of both untreated and PAA-treated cotton samples showed a shift of all crystallinity peaks toward slightly higher 2θ values, indicative of a decrease in interplanar distances (Fig. 9 and Table 4). Meanwhile, the degree of crystallinity of cellulose remained approximately constant. PAA treatment caused invariably a slight deformation of the crystalline parameters of cellulose, caused by the interactions arising between the hydrophilic, hydrogen bond-forming groups of cotton and PAAs, although with qualifications.

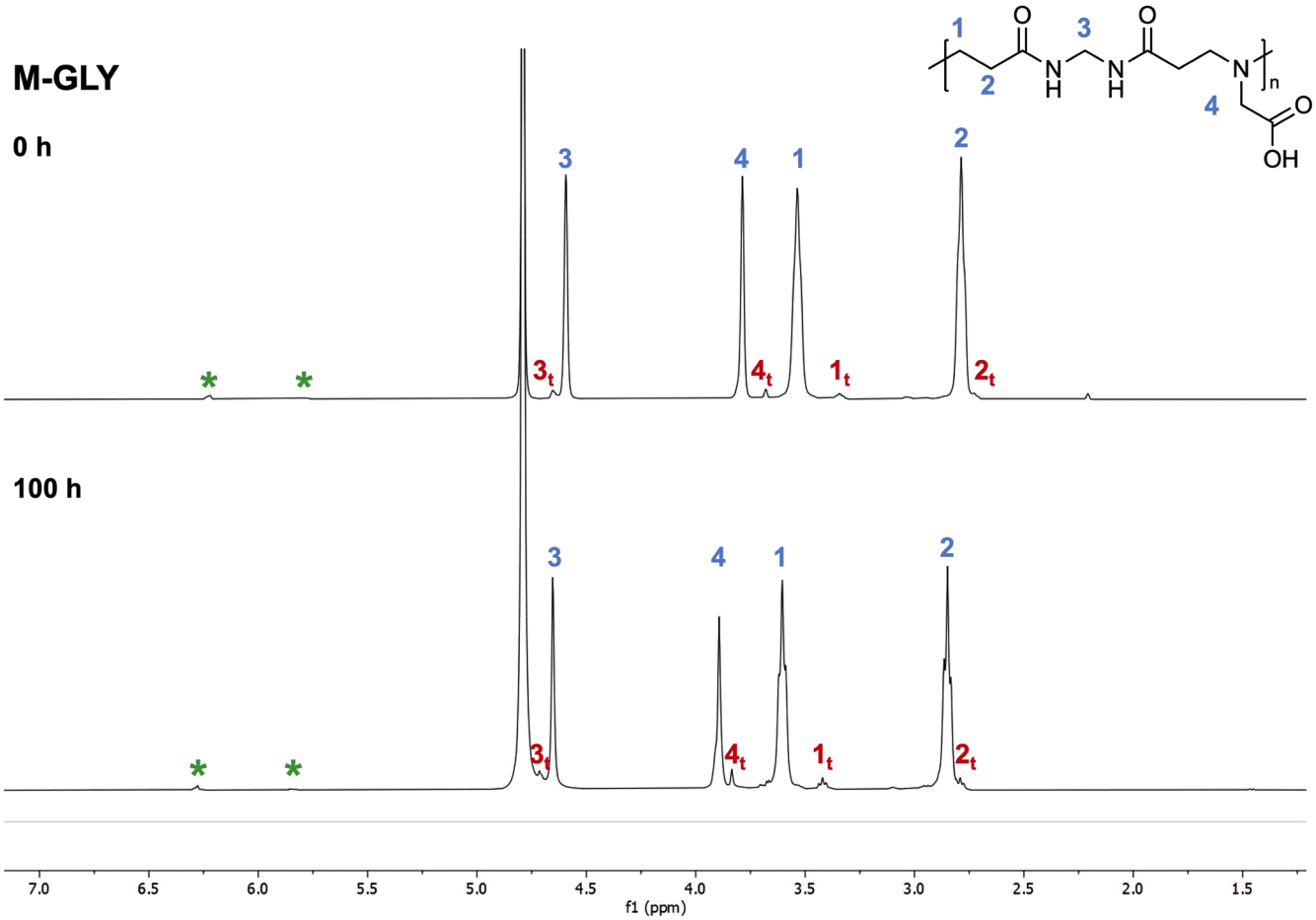

Fig. 10. ^{1}H-NMR spectra of M-GLY after 0 and 100 h UV irradiation.

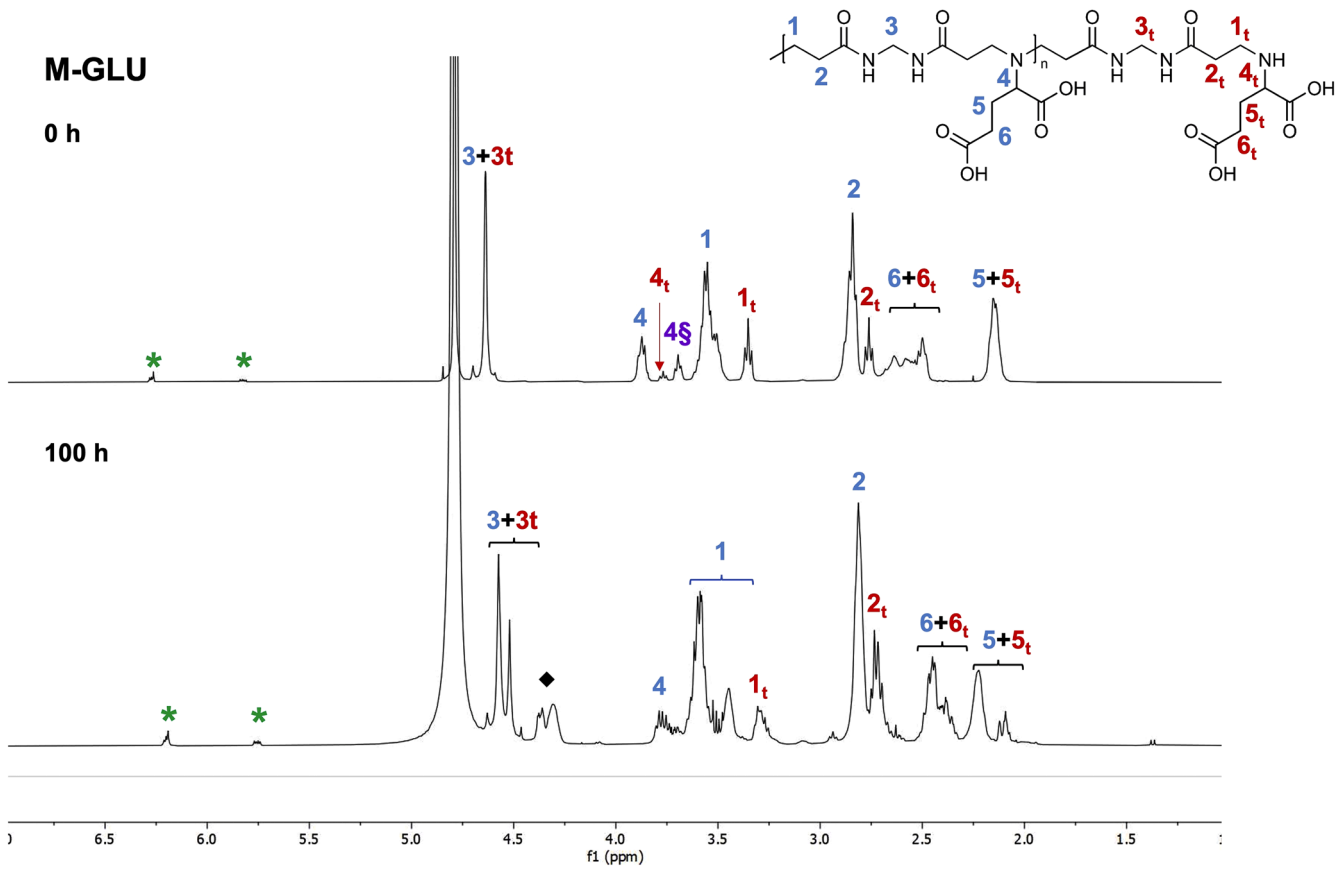

Fig. 11. [1]H-NMR spectra of M-GLU after 0 and 100 h UV irradiation. The green asterisks indicate traces of the vinyl-based terminals. The black rhomboidal bullet indicates unknown species. The purple tilde on peak n° 4 indicates differently protonated species. Small changes in the positions of the resonance peaks of the main chain hydrogens are due to the pH-dependence of the PAA proton magnetization.

The greatest differences of all were observed in M-ARG-treated and M-LEU-treated cotton, which showed a +0.60° and +0.86° shift, respectively, of the reference (110) peak. M-ARG was indeed the most greatly positively charged of the tested PAAs and M-LEU the most hydrophobic and most capable to diffuse within cellulose conformations. The shifts induced by the negatively charged M-GLU and M-GLY were not significant.

3.8. Analysis of PAA coatings and cotton after 100 h UV irradiation

At the end of the photoaging experiments, the PAA coatings were extracted with water from the impregnated cotton strips. The whiteness index values of the cotton strips subjected to water extraction were measured and compared with the values observed before impregnation with PAAs. The results collected (Table 5) demonstrate that after PAA extraction all cotton samples largely recovered the original whiteness. This result is in line with the fact that their FT-IR/ATR spectra were almost superimposable to that of untreated cotton (Fig. S10).

Meanwhile, the PAA aqueous solutions obtained after cotton extraction were freeze-dried and the resulting solid samples analyzed by [1]H-NMR spectrometry. The spectra of photoaged M-GLY (Fig. 10), M-LEU (Fig. S2) and M-ARG (Fig. S3) were superimposable to those of native PAAs after 0 h irradiation, demonstrating that no degradative phenomena occurred, and that no residues from cellulose decomposition were extracted.

Conversely, the spectrum of photoaged M-GLU (Fig. 11) significantly differs from that of native M-GLU after 0 h irradiation, indicating relevant structural changes, although not ascribed to backbone decomposition. In fact, the integrals of the resonance peaks of the methylene groups of the main chain, that is, protons 1, 2 and 3, are almost in the expected 1:1:1 ratio in the spectrum of photoaged M-GLU. Moreover, the small resonance peaks attributed to the acrylamide terminals (green asterisks in Fig. 11) do not increase in intensity, demonstrating that no depolymerization reaction occurred. The fact that peaks n° 4, 5 and 6, attributed to the methyne and methylene groups of the glutamic acid-derived pendants, change shape and intensity confirms that decomposition reaction involved the lateral groups. The observed structural changes could be ascribed, for instance, either to radical decarboxylation or cyclization reactions, or condensation with the decomposition fragments of cellulose. Noticeably, the singlet n° 3, that is, in the N,N'-methylenebisacrylamide-derived moiety, splits into two peaks in the spectrum of the photoaged sample.

4. Conclusions

The objective of this study was to evaluate the effectiveness as photostabilizers of cotton of a small group of α-amino acid-derived polyamidoamines, namely M-GLY, M-LEU, M-ARG and M-GLU, currently investigated as flame retardants for cotton. It was indeed hypothesized that they could exert a protective action against the photodegradation of cotton, since in both phenomena the degradation mechanism involves radical intermediates. Accelerated photoaging tests were conducted by subjecting cotton strips with 10% PAA add-on to UV irradiation in a closed chamber with reflecting surfaces, at controlled relative humidity (30%) and temperature varying from 25 to 50°C. Untreated cotton was treated in parallel as the control. All samples were irradiated for 4 h-cycles, then retrieved and analyzed by FT-IR spectroscopy, whiteness index and colorimetric tests. The total irradiation was 100 h. After 10–20 h, untreated cotton samples revealed an incipient light yellowing, almost visible to the naked eyes, whereas all PAA-

treated cotton samples did not visibly change color. Whiteness index and colorimetric parameters of cotton indicated significant yellowing already after 30 h irradiation, which slightly increased up to 100 h irradiation. The PAA-impregnated cotton strips showed a progressive but slower decrease of whiteness and increase of the yellow color, the latter always to a significantly lower extent compared to untreated cotton. In none of the cases analyzed did FT-IR analyses reveal detectable structural changes of cotton surface, both PAA-treated and untreated, even after 100 h irradiation. Scanning electron microscopy analysis showed moderate fraying of the cotton fibers in all tested samples after 100 h. TG analysis revealed that the thermogravimetric traces of the PAA-treated samples were unaffected by UV irradiation, whereas those of untreated cotton showed a slight increase of both the onset degradation temperature and the maximum degradation temperature, more significantly so in nitrogen than in air. After completion of the photoaging tests, PAAs were extracted with water from the aged PAA-treated cotton samples. All cotton fabrics almost completely recovered the original whiteness of untreated cotton before the start of photoaging, while the extracted PAAs showed no significant structural changes, as revealed by ^{1}H-NMR analysis, apart from the case of M-GLU, which showed structural alterations of the side groups. The efficacy of PAAs as photostabilizers was ascribed to their radical scavenger ability, due to the presence of the tert-amine groups their main chain. Interestingly, the data collected by colorimetric analyses revealed that the efficiency as cotton photostabilizer could be ranked as M-GLY ≈ M-ARG >> M-GLU > M-LEU. This trend could not be correlated to the different charge distribution of the PAAs, but rather to the presence in their repeating units of mobile hydrogens with different susceptibility to reactive radicals.

Overall, the reported results proved the potential of polyamidoamines derived from α-amino acids as anti-photoaging additives for cotton, allowing to predict that this property is not peculiar to only the PAAs presented in this study, but is rather a general property of this polymer family. This may pave the way for more extensive studies on PAA-based photostabilizers and on the correlations between effectiveness and structural features.

CRediT authorship contribution statement

Jenny Alongi: Writing – review & editing, Supervision, Conceptualization. **Sofia Treccani:** Methodology, Investigation. **Valeria Comite:** Investigation. **Paola Fermo:** Investigation. **Paolo Ferruti:** Writing – original draft, Conceptualization. **Elisabetta Ranucci:** Supervision, Funding acquisition, Conceptualization.

Declaration of competing interest

The authors declare that they have no known competing financial interests or personal relationships that could have appeared to influence the work reported in this paper.

Data availability

The data that has been used is confidential.

Acknowledgments

The Authors thank D. Pezzini (Politecnico di Torino) and S. Vitali (Università degli Studi di Milano) for the SEM observations and XRD experiments, respectively.

Supplementary materials

Supplementary material associated with this article can be found, in the online version, at doi:10.1016/j.polymdegradstab.2024.110938.

References

[1] J. Malešič, J. Kolar, M. Strlič, D. Kočar, D. Fromageot, J. Lemaire, O. Haillant, Photo-induced degradation of cellulose, Polym. Degrad. Stabil. 89 (2005) 64–69, https://doi.org/10.1016/j.polymdegradstab.2005.01.003.
[2] D.N.S. Hon, Photooxidative degradation of cellulose: Reactions of the cellulosic free radicals with oxygen, J. Polym. Sci. Polym. Chem. Ed. 17 (1979) 441–454, https://doi.org/10.1002/pol.1979.170170214.
[3] M. Baasandorj, D.K. Papanastasiou, R.K. Talukdar, A.S. Hassonc, J.B. Burkholder, $(CH_3)_3COOH$ (tert-butyl hydroperoxide): OH reaction rate coefficients between 206 and 375 K and the OH photolysis quantum yield at 248 nm, Phys. Chem. Chem. Phys. 12 (2010) 12101–12111, https://doi.org/10.1039/C0CP00463D.
[4] J. Kolar, Mechanism of autoxidative degradation of cellulose, Restaur. Int. J. Preserv. Libr. Arch. Mater. 18 (1997) 163–176, https://doi.org/10.1515/rest.1997.18.4.163.
[5] R. Hiatt, T. Mill, F.R. Mayo, Homolytic decompositions of hydroperoxides. I. Summary and implications for autoxidation, J. Org. Chem. 33 (1968) 1416–1420, https://doi.org/10.1021/jo01268a022.
[6] O.K. Alebeid, T. Zhao, Review on: developing UV protection for cotton fabric, J. Text. 108 (2017) 2027–2039, https://doi.org/10.1080/00405000.2017.1311201.
[7] K. Morabito, N.C. Shapley, K.G. Steeley, A. Tripathi, Review of sunscreen and the emergence of non-conventional absorbers and their applications in ultraviolet protection, Int. J. Cosmet. Sci. 33 (2011) 385–390, https://doi.org/10.1111/j.1468-2494.2011.00654.x.
[8] Y. Dobashi, J. Kondou, Y. Ohkatsu, Photo-antioxidant abilities of 2-hydroxybenzoyl compounds, Polym. Degrad. Stabil. 89 (2005) 140–144, https://doi.org/10.1016/j.polymdegradstab.2005.01.010.
[9] J.C. Suhadolnik, A.D. DeBellis, C. Hendricks-Guy, R. Iyengar, M.G. Wood, Unexpected electronic effects on benzotriazole UV absorber photostability: mechanistic implications beyond excited state intramolecular proton transfer, J. Coat. Technol. 74 (2002) 55–61, https://doi.org/10.1007/BF02720140.
[10] W. Czajkowski, J. Paluszkiewicz, R. Stolarski, M. Kaźmierska, E. Grzesiak, Synthesis of reactive UV absorbers, derivatives of monochlorotriazine, for improvement in protecting properties of cellulose fabrics, Dyes Pigments 71 (2006) 224–230, https://doi.org/10.1016/j.dyepig.2005.07.004.
[11] J.L. Hodgson, M.L. Coote, M.L. Coote, Clarifying the mechanism of the denisov cycle: how do hindered amine light stabilizers protect polymer coatings from photo-oxidative degradation? Macromolecules 43 (2010) 4573–4583, https://doi.org/10.1021/ma100453d.
[12] D.N.S. Hon, Stabilization of cotton fibers during mechanical cutting, Text. Res. J. 58 (1988) 575–580, https://doi.org/10.1177/004051758805801004.
[13] J. Struk-Sokołowska, J. Gwoździej-Mazur, Ł. Jurczyk, P. Jadwiszczak, U. Kotowska, J. Piekutin, F.A. Canales, B. Kaźmierczak, Environmental risk assessment of low molecule benzotriazoles in urban road rainwaters in Poland, Sci. Total Environ. 839 (2022) 156246, https://doi.org/10.1016/j.scitotenv.2022.156246.
[14] Y. Zhao, Y. Dan, Synthesis and characterization of a polymerizable benzophenone derivative and its application in styrenic polymers as UV-stabilizer, Eur. Polym. J. 43 (2007) 4541–4551, https://doi.org/10.1016/j.eurpolymj.2007.07.029.
[15] E. Ranucci, A. Manfredi, Polyamidoamines: versatile bioactive polymers with potential for biotechnological applications, Chem. Afr. 2 (2019) 167–193, https://doi.org/10.1007/s42250-019-00046-1.
[16] M. Arioli, A. Manfredi, J. Alongi, P. Ferruti, E. Ranucci, Highlight on the mechanism of linear polyamidoamine degradation in water, Polymers 12 (2020) 1–16, https://doi.org/10.3390/polym12061376.
[17] N. Mauro, F. Chiellini, C. Bartoli, M. Gazzarri, M. Laus, D. Antonioli, P. Griffiths, A. Manfredi, E. Ranucci, P. Ferruti, RGD-mimic polyamidoamine–montmorillonite composites with tunable stiffness as scaffolds for bone tis-sue-engineering applications, J. Tissue Eng. Regen. Med. 11 (2017) 2164–2175, https://doi.org/10.1002/term.2115.
[18] R. Cavalli, L. Primo, R. Sessa, G. Chiaverina, L. di Blasio, J. Alongi, A. Manfredi, E. Ranucci, P. Ferruti, The AGMA1 Po-lyamidoamine mediates the efficient delivery of SiRNA, J. Drug Target. 25 (2017) 891–898, https://doi.org/10.1080/1061186X.2017.1363215.
[19] P. Ferruti, J. Alongi, E. Barabani, A. Manfredi, E. Ranucci, Silk/Polyamidoamine membranes for removing chromium VI from water, Polymers 15 (2023) 1871, https://doi.org/10.3390/polym15081871.
[20] A. Manfredi, F. Carosio, P. Ferruti, E. Ranucci, J. Alongi, Linear polyamidoamines as novel biocompatible phosphorus-free surface confined intumescent flame retardants for cotton fabrics, Polym. Degrad. Stabil. 151 (2018) 52–64, https://doi.org/10.1016/j.polymdegradstab.2018.02.020.
[21] A. Beduini, F. Carosio, P. Ferruti, E. Ranucci, J. Alongi, Polyamidoamines derived from natural α-amino acids as effective flame retardants for cotton, Polymers 13 (2021) 3714, https://doi.org/10.3390/polym13213714.
[22] A. Beduini, F. Carosio, P. Ferruti, E. Ranucci, J. Alongi, Synergism between α-amino acid-derived polyamidoamines and sodium montmorillonite for enhancing the flame retardancy of cotton fabrics, Polym. Degrad. Stabil. 225 (2024) 110764, https://doi.org/10.1016/j.polymdegradstab.2024.110764.
[23] A. Beduini, F. Carosio, P. Ferruti, E. Ranucci, J. Alongi, Sulfur-based copolymeric polyamidoamines as efficient flame-retardants for cotton, Polymers 11 (2019) 1904, https://doi.org/10.3390/polym11111904.
[24] J. Alongi, A. Costantini, P. Ferruti, E. Ranucci, Evaluation of the eco-compatibility of polyamidoamines by means of seed germination test, Polym. Degrad. Stabil. 197 (2022) 109854, https://doi.org/10.1016/j.polymdegradstab.2022.109854.

[25] E. Ranucci, S. Treccani, P. Ferruti, J. Alongi, The seed germination test as a valuable tool for the short-term phytotoxicity screening of water-soluble polyamidoamines, Polymers 16 (2024) 1744, https://doi.org/10.3390/polym16121744.
[26] S. Treccani, P. Ferruti, J. Alongi, E. Monti, D. Zizioli, E. Ranucci, Ecotoxicity assessment of α-amino acid-derived polyamidoamines using zebrafish as a vertebrate model, Polymers 16 (2024) 2087, https://doi.org/10.3390/polym16142087.
[27] ISO 2469 Paper, Board and Pulps - Measurement of Diffuse Radiance Factor (Diffuse Reflectance Factor), International Organization for Standardization, Geneve, 2024.
[28] CIE15: Technical Report, 3rd ed., Colorimetry - CIELab.XYZ, 2004. https://cielab.xyz/pdf/cie.15.2004%20colorimetry.pdf.
[29] ISO 11664 Colorimetry, Part, 4: CIE 1976 L*a*b* Colour Space, International Organization for Standardization, Geneve, 2019.
[30] GZ. Schuessler 2024 https://zschuessler.github.io/DeltaE/learn/.
[31] F. Lazzari, A. Manfredi, J. Alongi, R. Mendichi, F. Ganazzoli, G. Raffaini, P. Ferruti, E. Ranucci, Self-structuring in water of polyamidoamino acids with hydrophobic side chains deriving from natural α-amino acids, Polymers 10 (2018) 1261, https://doi.org/10.3390/polym10111261.
[32] H. Jung, T. Sato, Comparison between the color properties of whiteness index and yellowness index on the CIELAB, Text. Color. Finish. 225 (2013) 241–246, https://doi.org/10.5764/TCF.2013.25.4.241.
[33] M. Jablonsky, J. Sima, Oxidative degradation of paper - A mini review, J. Cult. Herit. 48 (2021) 269–276, https://doi.org/10.1016/j.culher.2021.01.014.
[34] R. Davand, M.R. Rahimpour, S. Hassanajili, R. Rashedi, Theoretical and experimental assessment of UV resistance of high-density polyethylene: screening and optimization of hindered amine light stabilizers, J. Appl. Polym. Sci. 138 (2021) 51262, https://doi.org/10.1002/app.51262.
[35] A.D. French, Idealized powder diffraction patterns for cellulose polymorphs, Cellulose 21 (2014) 885–896, https://doi.org/10.1007/s10570-013-0030-4.
[36] H. Zhao, J.H. Kwak, Z.C. Zhang, H.M. Brown, B.W. Arey, J.E. Holladay, Studying cellulose fiber structure by SEM, XRD, NMR and acid hydrolysis, Carbohydr. Polym 68 (2007) 235–241, https://doi.org/10.1016/j.carbpol.2006.12.013.
[37] S. Park, J.O. Baker, M.E. Himmel, P.A. Parilla, D.K. Johnson, Cellulose crystallinity index: measurement techniques and their impact on interpreting cellulase performance, Biotechnol. Biofuels Bioprod. 3 (2010) 10. http://www.biotechnologyforbiofuels.com/content/3/1/10.